

# UC Davis

## UC Davis Previously Published Works

### Title

Heightened extended amygdala metabolism following threat characterizes the early phenotypic risk to develop anxiety-related psychopathology

### Permalink

<https://escholarship.org/uc/item/2z748849>

### Journal

Molecular Psychiatry, 22(5)

### ISSN

1359-4184

### Authors

Shackman, AJ  
Fox, AS  
Oler, JA  
[et al.](#)

### Publication Date

2017-05-01

### DOI

10.1038/mp.2016.132

Peer reviewed



Published in final edited form as:

*Mol Psychiatry*. 2017 May ; 22(5): 724–732. doi:10.1038/mp.2016.132.

## Heightened extended amygdala metabolism following threat characterizes the early phenotypic risk to develop anxiety-related psychopathology

Alexander J. Shackman<sup>a,b,c,\*</sup>, Andrew S. Fox<sup>d,e,f,g,h,i,\*</sup>, Jonathan A. Oler<sup>e,g,h</sup>, Steven E. Shelton<sup>e</sup>, Terrence R. Oakes<sup>j</sup>, Richard J. Davidson<sup>d,e,f,g,i</sup>, and Ned H. Kalin<sup>e,g,h,i,¶</sup>

<sup>a</sup>Department of Psychology, University of Maryland, College Park, MD 20742 USA

<sup>b</sup>Neuroscience and Cognitive Science Program, University of Maryland, College Park, MD 20742 USA

<sup>c</sup>Maryland Neuroimaging Center, University of Maryland, College Park, MD 20742 USA

<sup>d</sup>Department of Psychology, University of Wisconsin, Madison, WI 53719 USA

<sup>e</sup>Department of Psychiatry, University of Wisconsin, Madison, WI 53719 USA

<sup>f</sup>Center for Investigating Healthy Minds, University of Wisconsin, Madison, WI 53719 USA

<sup>g</sup>HealthEmotions Research Institute, University of Wisconsin, Madison, WI 53719 USA

<sup>h</sup>Lane Neuroimaging Laboratory, University of Wisconsin, Madison, WI 53719 USA

<sup>i</sup>Waisman Laboratory for Brain Imaging and Behavior, University of Wisconsin, Madison, WI 53719 USA

<sup>j</sup>inseRT MRI, Inc. Middleton, WI 53562 USA

### Abstract

Children with an anxious temperament (AT) are prone to heightened shyness and behavioral inhibition (BI). When chronic and extreme, this anxious, inhibited phenotype is an important early-life risk factor for the development of anxiety disorders, depression, and co-morbid substance abuse. Individuals with extreme AT often show persistent distress in the absence of immediate threat and this contextually inappropriate anxiety predicts future symptom development. Despite its clear clinical relevance, the neural circuitry governing the maladaptive persistence of anxiety remains unknown. Here, we used a well-established nonhuman primate model of childhood temperament and high-resolution <sup>18</sup>fluorodeoxyglucose positron emission

<sup>¶</sup>Please Address Correspondence to: Ned H. Kalin (nkalin@wisc.edu), Health Emotions Research Institute, Wisconsin Psychiatric Institute & Clinics, University of Wisconsin Madison, 6001 Research Park Boulevard, Madison, Wisconsin 53719 USA.

<sup>\*</sup>Equal authorship contributions

#### CONTRIBUTIONS

N.H.K. and S.E.S. designed the study. R.J.D. provided theoretical guidance. S.E.S. collected data. A.S.F. processed data. A.J.S., A.S.F., T.R.O., and N.H.K. analyzed data. A.S.F. and T.R.O. developed analytical tools. A.J.S., A.S.F., N.H.K., J.A.O., and R.J.D. contributed to data interpretation. A.J.S., A.S.F., and N.H.K. wrote the paper. A.J.S. and A.S.F. created figures and tables. N.H.K. supervised the study. All authors reviewed and revised the paper

#### CONFLICTS OF INTEREST

Authors declare no conflicts of interest.

tomography (FDG-PET) imaging to understand the neural systems governing persistent anxiety and clarify their relevance to early-life phenotypic risk. We focused on BI, a core component of anxious temperament, because it affords the moment-by-moment temporal resolution needed to assess contextually appropriate and inappropriate anxiety. From a pool of 109 peri-adolescent rhesus monkeys, we formed groups characterized by high or low levels of BI, as indexed by freezing in response to an unfamiliar human intruder's profile. The High-BI group showed consistently elevated signs of anxiety and wariness across more than 2 years of assessments. At the time of brain imaging, 1.5 years after initial phenotyping, the High-BI group showed persistently elevated freezing during a 30-min 'recovery' period following an encounter with the intruder — more than an order of magnitude greater than the Low-BI group — and this was associated with increased metabolism in the bed nucleus of the stria terminalis, a key component of the central extended amygdala. These observations provide a neurobiological framework for understanding the early phenotypic risk to develop anxiety-related psychopathology, for accelerating the development of improved interventions, and for understanding the origins of childhood temperament.

### Keywords

affective neuroscience; bed nucleus of the stria terminalis (BST); behavioral inhibition (BI); developmental psychopathology; extended amygdala; fear and anxiety; neuroimaging; temperament

---

When stable and extreme, anxious temperament is a prominent childhood risk factor for the development of anxiety disorders, depression, and co-morbid substance abuse<sup>1, 2</sup>. These disorders are common, debilitating, and challenging to treat<sup>3</sup>, highlighting the need to develop a deeper understanding of the neural systems that support elevated levels of dispositional anxiety and confer increased risk for the development of anxiety-related psychopathology.

Children with an anxious temperament often show sustained levels of heightened shyness, neuroendocrine activity, and behavioral inhibition (BI; e.g. freezing) in response to novelty and potential threat<sup>4, 5</sup>. Anxious temperament is a trait-like phenotype that is determined by a combination of heritable and non-heritable factors, evident early in life, decreased by the administration of anxiolytic agents, and expressed similarly in children and young monkeys<sup>4-8</sup>.

Persistent distress in the absence of immediate danger is a key feature of temperamental anxiety<sup>9, 10</sup>. Like adults<sup>11-13</sup>, children with extreme anxiety show potentiated defensive responses (e.g. startle) and report increased distress during periods of explicit safety before and after the presentation of threat<sup>14-18</sup>. Contextually inappropriate anxiety in the laboratory prospectively predicts heightened anxiety and exaggerated avoidance in the real world<sup>19, 20</sup>. Among adults with anxiety and depressive disorders, heightened 'spillover' and inertia of negative mood are common and predict the severity of clinical symptoms<sup>21, 22</sup>, the onset of future episodes of psychopathology<sup>23</sup>, and treatment response<sup>22</sup>.

Despite its clear clinical relevance, the neural circuitry governing the maladaptive persistence of anxiety in the minutes or hours following encounters with threat or other stressors remains poorly understood<sup>24</sup>. Recent work highlights the potential importance of the central extended amygdala, an anatomical concept encompassing the central (Ce) nucleus of the amygdala and the neighboring bed nucleus of the stria terminalis (BST). Mechanistic work in rodents indicates that the extended amygdala coordinates persistent defensive responses elicited by prolonged exposure to uncertain threat cues (e.g. cues paired with temporally unpredictable shock delivery) and diffusely threatening contexts (e.g. elevated-plus maze, brightly lit open field)<sup>11, 25–27</sup>. Imaging studies in monkeys demonstrate that activity in the extended amygdala predicts individual differences in freezing and other components of anxious temperament<sup>28, 29</sup>. Imaging studies in humans reveal increased activation in the dorsal amygdala in response to novel and potentially threatening faces among individuals with a childhood history of extreme BI<sup>5</sup>.

Here, we used a well-established nonhuman primate model of childhood anxiety and high-resolution <sup>18</sup>fluorodeoxyglucose (<sup>18</sup>FDG) positron emission tomography (PET) imaging to establish the contribution of the primate extended amygdala to persistently enhanced, context-inappropriate freezing during the ‘recovery’ period following an encounter with potential threat. We focused on freezing, a core component of the BI phenotype in children<sup>4, 30</sup> and the broader anxious temperament phenotype in monkeys<sup>5–7</sup>, because it affords the moment-by-moment temporal resolution needed to assess contextually appropriate and inappropriate anxiety. Young rhesus monkeys are ideal for understanding the neurobiology of extreme early-life anxiety. Reflecting the two species comparatively recent evolutionary divergence, the brains of rhesus monkeys and human children are genetically, anatomically, and functionally similar<sup>31, 32</sup>. This is important given known anatomical differences in the extended amygdala between rodents and primates<sup>33, 34</sup>. Homologous neurobiological substrates endow monkeys and humans with a shared repertoire of complex cognitive and socio-emotional behaviors and a common set of defensive responses to potential danger<sup>5, 7</sup>.

Adopting the longitudinal, extreme-groups strategy widely used to identify children at greatest risk<sup>1, 4</sup>, we phenotyped 109 peri-adolescent rhesus monkeys ( $M(SD)=2.19$  years (.50); range=1.45–3.42 years) on two occasions one week apart and formed groups with stable-high ( $n=11$ ; top quartile) or stable-low levels of BI ( $n=12$ ; bottom quartile) (Figures 1a, b). Here, the BI phenotype was quantified by measuring freezing in response to an unfamiliar human intruder’s profile (i.e. the ‘No Eye Contact’ condition of the Human Intruder Paradigm<sup>35</sup>), paralleling methods used in children<sup>7</sup>. To further assess the long-term stability and generality of the monkey BI phenotype, snake anxiety was assessed approximately 2 years after the initial phenotyping (Figure 1c).

A key advantage of the nonhuman primate model is that it permits concurrent measures of regional brain metabolism and naturalistic defensive responses. Here, the extreme BI groups were imaged on two occasions, more than 1.5 years after the initial phenotyping (Figure 1d). In the threat condition, subjects were placed in a testing cage and exposed to the human intruder’s profile for 30 min. Next, they received an injection of the radiotracer <sup>18</sup>FDG and were returned to the testing cage, where they were allowed to recover from the threat

encounter for 30 min. At the end of this ‘recovery’ period, subjects were anesthetized and placed in the PET scanner. The control condition differed only in the absence of threat exposure during the initial 30-min. Comparison of the physically-identical ‘recovery’ phases of the threat and control conditions enabled us to assess persistent group differences in freezing and accompanying brain activity. In contrast to conventional functional MRI techniques, FDG-PET, which provides a measure of regional brain metabolism integrated over the 30-minute ‘recovery’ period, is uniquely well suited for assessing sustained neural responses<sup>36</sup>. Establishing the neural systems that support persistent, contextually inappropriate anxiety is important for understanding the mechanisms that contribute to the development and maintenance of psychopathology, for guiding the development of improved prevention and treatment strategies, and for understanding the neural bases of childhood temperament.

## METHODS AND MATERIALS

### Subjects

Peri-adolescent rhesus monkeys (*Macaca mulatta*;  $n=109$ ; 63.3% female;  $M(SD)=2.19$  years (.50); range=1.45–3.42 years) were tested as part of a larger program of research to understand the mechanisms underlying early-life anxiety<sup>6, 37–39</sup>. Data were collected between September 2004 and November 2006. Hypothesis testing focused on data obtained from 23 animals selected on the basis of stable and extreme levels of freezing (High-BI:  $n=11$ ; Low-BI:  $n=12$ ; Table 1). We focused on freezing because, in contrast to other components of anxious temperament phenotype (e.g. cortisol), it affords the temporal resolution needed to dissociate recovery from the acute impact of exposure to the intruder’s profile (cf. Figure 1d). The procedures used for forming extreme groups are detailed below. In contrast to post-hoc dichotomization, the use of extreme groups is scientifically and statistically appropriate, given our focus on stable and extreme levels of BI<sup>40</sup>. Prior work by our group using similar extreme-groups designs indicates adequate power to detect mean differences with 11–12 animals per group (e.g. 92.9% power to detect  $d=1.5$  using two-tailed  $\alpha=.05$ )<sup>41, 42</sup>. All procedures were in accord with guidelines established by the local Institutional Animal Care and Use Committee.

### General Procedures

All techniques have been described in detail in prior publications by our group<sup>6, 37–39</sup>. Experimental personnel were blind to group status at the time of data collection. For additional details, see the Supplement.

### Formation of Groups with Stable and Extreme BI

Research in children indicates that those who consistently express high levels of BI (e.g. more persistent freezing, fewer vocalizations) across repeated assessments are at the greatest risk for the development of psychopathology<sup>1, 43</sup>. Accordingly, groups with stable, extreme levels of the BI phenotype were formed by organizing animals into quartiles based on log<sub>10</sub>-transformed freezing during exposure to the human intruder’s profile for the first, second, and mean of the two phenotyping sessions (Figure 1a). Individual differences in intruder-elicited freezing were continuously distributed without obvious gaps or discontinuities

(Supplementary Figure S1), consistent with prior work by our group<sup>28</sup>. Subjects who remained in the same quartile across the three metrics were deemed stable. Age- and sex-matched groups were formed using the most extreme individuals with stable phenotypes. During the initial phenotyping sessions, freezing was also assessed in the absence of potential threat (i.e. the 'Alone' condition of the Human Intruder Paradigm<sup>7, 35</sup>; Figure 1a). The Alone condition was always administered first to circumvent carry-over from the higher-intensity intruder challenge

### Snake Anxiety

To clarify the stability and generality of the BI phenotype, snake anxiety was assessed using standard techniques<sup>42</sup> (see the Supplement) ~2 years after initial phenotyping (Figure 1c). Subjects were pre-trained to retrieve preferred foods. During the assessment, foods were placed on top of a transparent enclosure containing a live snake, comparison stimuli (i.e. artificial snake, roll of tape), or nothing (6 trials/condition; order counterbalanced). Because many subjects refused to respond in the presence of the live snake (55% and 17% of the High- and Low-BI groups, respectively), anxiety was assessed using the total number of non-responses (square-root transformed), circumventing the need to omit subjects with incomplete response time (RT) data and maximizing statistical power.

### FDG-PET and MRI Data Acquisition

Brain FDG metabolism was measured on two occasions (i.e. the threat and control conditions depicted in Figure 1d) ~1.5 years after the phenotyping sessions ( $M(SD)$  interval=1.62 (.06) years; Table 1). The order of the two FDG-PET sessions was pseudo-randomized across subjects and balanced across groups. Imaging sessions occurred within 28 days of one another ( $M=2.20$  weeks,  $SD=1.10$ ). Subjects were acclimated to the imaging procedures prior to the first FDG-PET session (see the Supplement). FDG-PET reflects the amount of regional FDG uptake and metabolism between the injection and PET scan, with majority of uptake occurring in the first 30 min. Anatomical scans were collected using a GE Signa 3T MRI scanner, standard quadrature coil, and a 3D T1-weighted, inversion-recovery, gradient-echo prescription (TI/TR/TE/Flip/NEX/FOV/Matrix/Bandwidth/Slices/Gap:600ms/8.648ms/1.888ms/10°/2/140mm/256×224/61.0547kHz/128/-0.5mm; reconstructed to 0.2734×0.2734×0.5 mm). Brain activity during the first half of the session (Figure 1d), prior to FDG administration, was not measured.

### Brain Imaging Data Processing Pipeline

As detailed in the Supplement, T1-weighted anatomical images and FDG-PET data were normalized to a study-specific rhesus template (0.625-mm<sup>3</sup>) using standard techniques. Anatomical images were segmented using FAST (<http://www.fmrib.ox.ac.uk/fsl/fast4>). PET and gray matter probability maps were smoothed 4mm.

### Hypothesis Testing Strategy

Brain and behavioral data were carefully inspected to ensure that inferential test assumptions were adequately satisfied. As detailed in the Supplement, we used a series of voxelwise general linear models (GLM) to identify regions (i) where the Group (High-BI, Low-BI) ×

Condition (Alone-Following-Intruder, Alone-Following-Alone) interaction was significant and (ii) where the High-BI group showed significantly more metabolism than the Low-BI group during the critical 30-min ‘recovery’ period following the threat encounter (Alone-Following-Intruder). Given our *a priori* focus on the contributions of the extended amygdala, each test was thresholded at  $p < .05$ , corrected for a region-of-interest (ROI) encompassing the amygdala, BNST, and substantia innominata. To identify regions satisfying both of these key criteria, thresholded maps were combined using a minimum conjunction (logical AND)<sup>44</sup>, as in prior work by our group<sup>28</sup>. To provide additional information about specificity, clusters lying outside of the ROI that survived the small-volume threshold are depicted visually and detailed in the supplementary tables (i.e. were not masked). On an exploratory basis, we also assessed whether they survived a whole-brain, cluster-extent threshold. The code and scripts used to conduct these analyses is available upon request.

## RESULTS

### Identifying Stable and Extreme BI Groups

Across the two phenotyping sessions (Figure 1a), the screening sample of 109 individuals spent more than an order of magnitude more time freezing in response to the human intruder’s profile compared to when they were alone in the testing cage (Intruder:  $M(SD)=161.6$  seconds (112.6); Alone:  $M(SD)=14.1$  seconds (24.5)),  $F(1,108)=484.09$ ,  $p < .001$ ). For detailed results, see the Supplement. Individual differences in intruder-elicited freezing were stable over the one week interval,  $r=.74$ ,  $p < .001$  (Figure 1b). Using these data, we formed sex- and age-matched groups with stable and extreme levels of the BI phenotype (High-BI, Low-BI; see Tables 1 and S1).

When compared to the Low-BI group, the High-BI group showed an 18-fold increase in freezing when the human intruder was present. Additional analyses revealed a 13-fold increase when the High-BI individuals were alone in the testing cage at the beginning of the session ( $(F(1,21)=8.56$ ,  $p=.008$ ; see Figure 1a and Table S1). In other words, although BI is more strongly expressed in response to the intruder’s profile (Group  $\times$  Context interaction:  $F(1,21)=13.73$ ,  $p=.001$ ; note: this  $p$ -value should be interpreted with caution, as this test is not independent of the group-selection procedures), it also manifests in response to the diffusely threatening testing cage.

### The BI Phenotype Shows Continuity Across Time and Contexts

To gauge the long-term stability and generality of the BI phenotype, we performed two additional analyses. First, we tested whether the High-BI group continued to show elevated freezing during the first 30 minutes of the imaging sessions, prior to FDG administration (see Figure 1d). Analyses revealed that subjects froze more in response to the intruder’s profile ( $F(1,21)=9.41$ ,  $p=.006$ ) and that the High-BI group froze substantially more than the Low-BI group, ( $F(1,21)=10.12$ ,  $p=.004$ ; Table S2). In fact, the High-BI group froze more than 8 times longer than the Low-BI group when the intruder was present ( $F(1,21)=10.61$ ,  $p=.004$ ) and nearly 5 times longer when they were alone in the testing cage ( $F(1,21)=4.99$ ,  $p=.04$ ), despite extensive acclimation to both the cage and testing procedures (see the Supplement). Across groups, individual differences in the BI phenotype (i.e. intruder-



elicited freezing) exhibited substantial test-retest reliability ( $ICC=.85$ ) over the ~1.5 years separating the phenotyping from the brain imaging sessions (Figure 1).

As a second test of phenotypic continuity, we assessed snake anxiety ~2 years after the initial phenotyping sessions (Figure 1c). Analyses revealed a significant effect of Stimulus on anxiety ( $F(3,63)=30.11$ ,  $p<.001$ ). In particular, the frequency of non-responses followed the expected linear pattern: Live Snake > Artificial Snake > Tape > Nothing ( $F(1,21)=62.56$ ,  $p<.001$ ) and all of the pairwise differences between stimuli were in the expected direction and significant ( $ps<.03$ ). Importantly, the Group  $\times$  Stimulus interaction was also significant ( $F(1,21)=2.83$ ,  $p<.05$ ). The High-BI group was twice as likely to refrain from reaching for a highly preferred food reward in the presence of the live snake compared to the Low-BI group ( $F(1,21)=5.76$ ,  $p=.03$ ). Other differences were not significant ( $ps>.20$ ). Analyses of observer ratings of freezing behavior during the snake anxiety assessment revealed a similar pattern (Supplement and Table S2). Across groups, reticence in the presence of the live snake was prospectively predicted by individual differences in freezing to the intruder's profile during the phenotyping sessions more than 2 years earlier ( $\rho_{Spearman}=.44$ ,  $p=.04$ ,  $n=23$ ). Collectively, these results indicate that the monkey BI phenotype represents an enduring predisposition to respond to a range of potentially threatening cues and contexts with heightened anxiety.

### The High-BI Group Shows Persistently Elevated Freezing Following the Intruder Encounter

Next, we tested whether the High-BI group exhibits persistently elevated freezing following the encounter with the human intruder. Analyses revealed that, on average, subjects froze longer following the intruder encounter ( $F(1,21)=8.20$ ,  $p=.009$ ; Fig. 2b and Table S2). Consistent with expectation, the Group  $\times$  Condition interaction was significant ( $F(1,21)=4.62$ ,  $p=.04$ ). Pairwise contrasts revealed that the High-BI group froze significantly longer during the Alone-Following-Intruder condition compared to the Alone-Following-Alone condition ( $F(1,21)=12.04$ ,  $p=.002$ ), whereas the Low-BI group did not show significant differences in freezing ( $p=.61$ ). This effect was specific to the 'recovery' period following the termination of threat: the High-BI group froze an order of magnitude longer than the Low-BI group during the Alone-Following-Intruder condition ( $F(1,21)=6.61$ ,  $p=.02$ ), whereas the groups did not significantly differ during the Alone-Following-Alone condition ( $p=.35$ ). The main effect of Group was not significant ( $p=.08$ ). These results demonstrate that individuals with stable and extreme BI show sustained levels of heightened anxiety during the half-hour following the intruder encounter.

### The High-BI Group Shows Elevated Activity in the BST Region Following the Intruder Encounter

To identify the neural systems underlying group differences in freezing following the intruder encounter, we used a whole-brain voxelwise GLM to identify regions where the critical Group  $\times$  Condition interaction was significant in the period following FDG administration (Figure 1d). Given our *a priori* focus on the extended amygdala, the interaction was thresholded at  $p<.05$  (corrected for a 4,188-voxel region-of-interest [ROI] encompassing the amygdala and BST; depicted in green in Figure 3). This analysis revealed a cluster in the region of the BST (Figure 3a; Table S3; Supplementary Figure S2). We used



a second whole-brain analysis to identify regions where the High-BI group showed significantly more activity than the Low-BI group during the Alone-Following-Intruder condition ( $p < .05$ , corrected). This revealed an overlapping cluster within the *a priori* ROI (Figure 3b; Table S4). Although several clusters were significant in one or the other of these two statistical maps, the region of overlap in the region of the BST was the only cluster in the entire brain to satisfy both of these critical tests (Figures 3c–e and Supplementary Figure S3). This effect was specific to the period following threat; like freezing behavior, the High- and Low-BI groups did not show significant differences in activity in the BST or other parts of the extended amygdala during the control condition (Alone-Following-Alone; cf. Figure 3e).

Compared to other brain regions implicated in BI and anxiety, the BST is small and lacks distinct macroscopic boundaries<sup>33</sup>, making it challenging to definitively localize using conventional brain imaging techniques. To better understand the region showing elevated activity in the High-BI group (purple cluster in Figure 3c), we capitalized on work demonstrating that the BST and Ce show robust anatomical<sup>33</sup> and functional connectivity<sup>45</sup>. Here we used previously published<sup>45</sup> fMRI data obtained from an independent sample of 89 young monkeys to demonstrate that the hyper-metabolic cluster identified using FDG-PET overlaps with a region expressing high levels of ‘resting-state’ functional connectivity with the Ce (Figure 4; significant connectivity depicted in green; overlap depicted in purple), enhancing our confidence that it includes the BST.

To clarify the consequences of elevated BST metabolism, we extracted activity from the region of overlap identified using FDG-PET (Figure 3c) for each subject and assessed brain-behavior relations after controlling for nuisance variance in mean-centered gray matter probability. Consistent with the group mean differences described above, individual differences in BST activity following the intruder encounter (a) were prospectively predicted by intruder-elicited freezing during the initial phenotyping sessions (partial  $\rho = .58$ ,  $p = .005$ ), (b) predicted concurrent freezing (partial  $\rho = .46$ ,  $p = .03$ ), and (c) discriminated High-BI individuals with good sensitivity (90.9%) and specificity (83.3%),  $\chi^2(1) = 15.51$ ,  $p < .001$ . These relations were specific to the period following the encounter with potential threat; significant associations were not obtained using BST activity associated with the Alone-Following-Alone control condition ( $ps > .20$ ). Collectively, these findings suggest that elevated activity in the BST plays a key role in promoting extreme early-life anxiety.

## DISCUSSION

The present study, which combines longitudinal phenotyping with high-resolution FDG-PET imaging in young nonhuman primates, provides unique insights into the neural bases of extreme early-life anxiety. Consistent with research in children and adolescents, this work demonstrates that BI represents a trait-like tendency to respond to a range of potentially threatening cues and contexts with increased signs of anxiety. Drawing from a pool of 109 young monkeys, we formed age- and sex-matched groups characterized by stable and extreme freezing in response to an unfamiliar human intruder (Figures 1a, b). Compared to the Low-BI group, the High-BI group showed nearly twenty times more freezing to the intruder during the two screening sessions and an order of magnitude more freezing when

they re-encountered the intruder ~1.5 years later. The High-BI group also showed increased reticence when exposed to a snake ~2 years after the initial phenotyping sessions (Figure 1c and Supplement). In short, the BI phenotype shows continuity across time and across different types of ethologically relevant threats in young monkeys. Importantly, the High-BI group also showed increased freezing when alone in the testing cage during the initial phenotyping sessions and continued to show exaggerated wariness and inhibition in the testing cage during the first 30 min of the brain imaging sessions (i.e. prior to FDG administration), despite repeated exposure to this context during the intervening year-and-a-half. These observations suggest that extreme BI manifests in amplified caution and anxiety in situations where threat is diffuse, weak, or uncertain. Consistent with this perspective, the High-BI group showed persistently elevated freezing during the 30-min recovery period following the intruder encounter (Figure 2b)—more than an order of magnitude greater than the Low-BI group—and this was associated with increased metabolic activity in the BST region (Figures 3, 4). Hyper-metabolism was associated with exaggerated freezing and discriminated High- and Low-BI individuals with good sensitivity and specificity. Collectively, these observations provide compelling evidence that sustained levels of heightened anxiety in the absence of immediate threat reflect elevated activity in the BST region.

In children, anxious temperament and the narrower BI phenotype are heritable early-life risk factors for the development of anxiety, depression, and co-morbid substance abuse<sup>1, 2, 5</sup> and our results provide a neurobiologically-grounded framework for understanding the mechanisms underlying this liability. In particular, our results provide evidence that individuals with consistently high levels of the BI phenotype early in development show persistent wariness in the period following exposure to potential threat and that this is associated with increased engagement of the BST. These observations complement evidence that threat-elicited activity in the BST is heritable and genetically correlated with individual differences in anxious temperament in young monkeys<sup>29</sup>. The relevance of the BST to sustained anxiety is consistent with anatomical tracing studies in rodents and monkeys showing that this region sends dense projections to brainstem and subcortical effector sites<sup>33, 46</sup>. Our imaging results are also consistent with mechanistic studies in rodents showing that the BST exhibits persistent excitability following direct stimulation, supports passive avoidance during sustained exposure (5–20 min.) to diffusely threatening contexts (e.g. elevated-plus maze), and contributes to the over-generalization of anxiety to safety cues (CS-)<sup>11, 25, 26, 47, 48</sup>.

Our observations provide an important extension of recent imaging work documenting that: (a) individuals with extreme anxiety show elevated activation in the vicinity of the BST during exposure to uncertain threat and punishment<sup>49–52</sup> and (b) individual differences in BST function predict anxious mood, freezing, skin conductance, and cortisol elicited by uncertain or diffuse threat<sup>6, 28, 29, 38, 53–56</sup>. Extending earlier work in rodents, monkeys, and humans, our results reflect the comparison of two physically-identical conditions (i.e. Alone-Following-Intruder and Alone-Following-Alone; Figure 1d), neural activity integrated over an extended 30 min ‘recovery’ period following the offset of threat, concurrent measures of naturalistic defensive responses in individuals selected on the basis of stable and

extreme phenotypic risk, and a multi-modal imaging approach to identifying the BST region. These features enhance our confidence in the translational significance of these results.

While the BST has not been previously linked to childhood BI, our findings dovetail with emerging evidence that, like anxious adults<sup>9, 11–13</sup>, children and adolescents with a history of extreme BI and elevated anxiety are prone to contextually inappropriate defensive behaviors<sup>14–18, 57</sup>. Moreover, contextually inappropriate responses in the laboratory prospectively predict heightened real-world anxiety in children and avoidance of threat-related contexts in adults<sup>19, 20</sup>. Among adults, heightened apprehension and defensive responses in safe contexts are generally more discriminative of pathological anxiety than that elicited by overt threat<sup>11, 12</sup>. This maladaptive phenotype appears to be amplified by early adversity<sup>58</sup> and prospectively predicts the onset of anxiety disorders in adolescence<sup>59</sup> as well as the intensification of anxious symptoms in young adults<sup>60</sup>. Collectively, these findings underscore the potential etiological significance of heightened BST activity.

The BST is increasingly conceptualized as a key promoter of ‘sustained’ defensive responses to uncertain, psychologically diffuse, or temporally remote threat and our results are broadly consistent with this perspective. Nonetheless, it is likely that the BST makes a broader contribution to phenotypic risk and anxiety, one that encompasses exaggerated defensive responses during both sustained and transient exposure to uncertain threat<sup>33, 61</sup>. Mechanistic work in rodents suggests that BST engagement can begin quite early, between 4 and 60 s following the onset of cues associated with uncertain danger<sup>11</sup>, and contributes to the overgeneralization of conditioned fear to 30 s auditory cues<sup>25</sup>. In human fMRI studies, BST activation has also been observed in response to acute aversive challenges (e.g. 4-s tarantula video clip; see Refs. <sup>62–65</sup>). In fact, a recent meta-analysis demonstrated that imaging studies of fear and anxiety consistently reveal activation in the region of the central extended amygdala, including the BST as well as the Ce, across a broad spectrum of populations, paradigms, and time-scales<sup>33</sup>. An important avenue for future research will be to clarify the boundary conditions and mechanistic importance of BST engagement. Likewise, while our results highlight the importance of the BST, it will be important to understand how functional interactions between the BST and other regions sensitive to potential threat (e.g. Ce, periaqueductal gray, orbitofrontal cortex, insula, and anterior cingulate) control the expression of persistent anxiety, support variation in early phenotypic risk, and ultimately contribute to the development and maintenance of psychopathology in humans<sup>24, 29, 54, 66–68</sup>. Given the higher prevalence of anxiety disorders and depression among women<sup>69, 70</sup>, understanding potential sex differences in the function of these circuits and their relevance to risk represents another key challenge.

As we and other commentators have recently noted, understanding the BST is challenging<sup>33, 71</sup>. From a technical standpoint, the BST is small; it is functionally and anatomically heterogeneous; and it lacks clear boundaries *in vivo*, even when using ultra-high field-strength MRI techniques<sup>33, 72, 73, 74, 75</sup>. Furthermore, most imaging software for automated cluster labeling does not include the BST, although standardized segmentation protocols<sup>75</sup> and masks have recently become available (<https://afni.nimh.nih.gov/afni/community/board/read.php?1,149436,149436>). The upshot is that researchers may not recognize that a cluster encompasses the BST or may be hesitant to label it as such.

Regardless of the label, there is value to discussing the potential role of the BST and other neighboring regions of the basal forebrain (e.g. accumbens), even in cases where a cluster cannot be unambiguously ascribed to the BST. Using multi-band imaging sequences and high-precision spatial normalization techniques would provide enhanced spatial resolution<sup>29, 76</sup>. Multi-modal ‘double-labeling’ strategies, as in the present study (i.e. FDG-PET paired with resting-state fMRI) and other recent work by our group<sup>29</sup> (i.e. FDG-PET paired with *in vivo* dopamine receptor imaging) provide other tools for ascertaining whether a cluster is likely to include the BST.

Our results also have implications for theories of temperament and personality<sup>9, 77</sup>. There is ample evidence that individuals who are most at risk for developing a mood or anxiety disorder are prone to persistently elevated distress in contexts where threat is distant or absent<sup>78, 79</sup>. In fact, longitudinal experience-sampling studies suggest that the vast majority of negative affect experienced by adults with an anxious disposition cannot be attributed to clear-cut stressors in the immediate environment<sup>80</sup>. Although this has been described as a tonic or endogenous effect of temperament<sup>78</sup>, our results suggest that it may reflect increased reactivity to stressors that are weak, diffuse (cf. the test cage) or temporally remote (cf. the Alone-Following-Intruder condition). Our results and others<sup>33</sup> motivate the hypothesis that this pervasive anxiety partially reflects alterations in BST function.

## CONCLUSIONS

The present study demonstrates that individuals with stable and extreme BI respond to a range of potentially threatening cues and contexts with exaggerated defensive responses. Young monkeys with elevated levels of BI consistently over-reacted to both overt and more diffuse kinds of threat during more than two years of longitudinal study. Concurrent measures of FDG metabolism provide unique evidence that heightened defensive responses following an encounter with potential threat reflects increased engagement of the BST, a key component of the central extended amygdala. The present study has several features that enhance our confidence in the translational significance of these results, including the use of a well-validated primate model of early-life anxiety, physically identical ‘recovery’ conditions<sup>81, 82</sup>, concurrent measures of evolutionarily-conserved emotional behaviors, and a multi-modal approach to identifying the BST. Translational brain imaging strategies, like that featured in the present study, provide a powerful tool for bridging the gap separating the mechanistic insights afforded by nonhuman animal models from the complexity of human emotions, temperament, and psychopathology and accelerating therapeutic development. Developing more effective interventions is particularly important for minimizing the cumulative damage associated with extreme BI and anxiety early in development.

## Supplementary Material

Refer to Web version on PubMed Central for supplementary material.

## Acknowledgments

Authors acknowledge assistance and critical feedback from A. Alexander, A. Converse, L. Friedman, D. Grupe, R. Hoks, T. Johnson, S. Mansavage, K. Meyer, L. Pessoa, D. Pine, P. Rudebeck, W. Shelledy, M. Stockbridge, T.

Johnstone, E. Zao, and the staffs of the Harlow Center for Biological Psychology, HealthEmotions Research Institute (HERI), and Wisconsin National Primate Center. We are particularly grateful for the contributions of Helen Van Valkenberg to this work. This work was supported by the National Institutes of Health (HD003352, HD008352, MH018931, MH046729, MH069315, MH081884, MH084051, MH091550, MH107444, OD011106, and RR000167), HERI, Meriter Hospital, and University of Maryland.

## References

1. Clauss JA, Blackford JU. Behavioral inhibition and risk for developing social anxiety disorder: a meta-analytic study. *J Am Acad Child Adolesc Psychiatry*. 2012; 51:1066–1075. [PubMed: 23021481]
2. Pine DS, Fox NA. Childhood antecedents and risk for adult mental disorders. *Annu Rev Psychol*. 2015; 66:459–485. [PubMed: 25559116]
3. Insel TR. Next-generation treatments for mental disorders. *Science translational medicine*. 2012; 4:155ps119.
4. Kagan J, Reznick JS, Snidman N. Biological bases of childhood shyness. *Science*. 1988; 240:167–171. [PubMed: 3353713]
5. Fox AS, Kalin NH. A translational neuroscience approach to understanding the development of social anxiety disorder and its pathophysiology. *Am J Psychiatry*. 2014; 171:1162–1173. [PubMed: 25157566]
6. Fox AS, Shelton SE, Oakes TR, Davidson RJ, Kalin NH. Trait-like brain activity during adolescence predicts anxious temperament in primates. *PLoS ONE*. 2008; 3:e2570. [PubMed: 18596957]
7. Oler, JA., Fox, AS., Shackman, AJ., Kalin, NH. The central nucleus of the amygdala is a critical substrate for individual differences in anxiety. In: Amaral, DG., Adolphs, R., editors. *Living without an amygdala*. Guilford; NY: 2016.
8. Buss, KA., Kiel, EJ. Temperamental risk factors for pediatric anxiety disorders. In: Vasa, RA., Roy, AK., editors. *Pediatric anxiety disorders: A clinical guide*. Springer; NY: 2013. p. 47-68.
9. Shackman, AJ., Stockbridge, MD., LeMay, EP., Fox, AS. The psychological and neurobiological bases of dispositional negativity. In: Fox, AS.Lapate, RC.Shackman, AJ., Davidson, RJ., editors. *The nature of emotion. Fundamental questions. 2*. Oxford University Press; NY: in press
10. Davidson RJ, Jackson DC, Kalin NH. Emotion, plasticity, context, and regulation: Perspectives from affective neuroscience. *Psychol Bull*. 2000; 126:890–909. [PubMed: 11107881]
11. Davis M, Walker DL, Miles L, Grillon C. Phasic vs sustained fear in rats and humans: Role of the extended amygdala in fear vs anxiety. *Neuropsychopharmacology*. 2010; 35:105–135. [PubMed: 19693004]
12. Duits P, Cath DC, Lissek S, Hox JJ, Hamm AO, Engelhard IM, et al. Updated meta-analysis of classical fear conditioning in the anxiety disorders. *Depress Anxiety*. 2015:239–253. [PubMed: 25703487]
13. Grupe DW, Nitschke JB. Uncertainty and anticipation in anxiety: an integrated neurobiological and psychological perspective. *Nat Rev Neurosci*. 2013; 14:488–501. [PubMed: 23783199]
14. Barker TV, Reeb-Sutherland BC, Fox NA. Individual differences in fear potentiated startle in behaviorally inhibited children. *Dev Psychobiol*. 2014; 56(1):133–141. [PubMed: 23341151]
15. Reeb-Sutherland BC, Helfinstein SM, Degnan KA, Perez-Edgar K, Henderson HA, Lissek S, et al. Startle response in behaviorally inhibited adolescents with a lifetime occurrence of anxiety disorders. *J Am Acad Child Adolesc Psychiatry*. 2009; 48:610–617. [PubMed: 19454917]
16. Waters AM, Nazarian M, Mineka S, Zinbarg RE, Griffith JW, Naliboff B, et al. Context and explicit threat cue modulation of the startle reflex: preliminary evidence of distinctions between adolescents with principal fear disorders versus distress disorders. *Psychiatry Res*. 2014; 217:93–99. [PubMed: 24679992]
17. Jovanovic T, Nylocks KM, Gamwell KL, Smith A, Davis TA, Norrholm SD, et al. Development of fear acquisition and extinction in children: effects of age and anxiety. *Neurobiol Learn Mem*. 2014; 113:135–142. [PubMed: 24183838]
18. Reznick JS, Kagan J, Snidman N, Gersten M, Baak K, Rosenberg A. Inhibited and uninhibited children: A follow-up study. *Child Dev*. 1986; 57:660–680.

19. Buss KA, Davis EL, Kiel EJ, Brooker RJ, Beekman C, Early MC. Dysregulated fear predicts social wariness and social anxiety symptoms during kindergarten. *J Clin Child Adolesc Psychol.* 2013; 42:603–616. [PubMed: 23458273]
20. Grillon C. Associative learning deficits increase symptoms of anxiety in humans. *Biol Psychiatry.* 2002; 51:851–858. [PubMed: 12022957]
21. Houben M, Van Den Noortgate W, Kuppens P. The relation between short-term emotion dynamics and psychological well-being: A meta-analysis. *Psychol Bull.* 2015
22. Newman MG, Fisher AJ. Mediated moderation in combined cognitive behavioral therapy versus component treatments for generalized anxiety disorder. *J Consult Clin Psychol.* 2013; 81:405–414. [PubMed: 23398493]
23. van de Leemput IA, Wichers M, Cramer AO, Borsboom D, Tuerlinckx F, Kuppens P, et al. Critical slowing down as early warning for the onset and termination of depression. *Proc Natl Acad Sci U S A.* 2014; 111(1):87–92. [PubMed: 24324144]
24. Tovote P, Fadok JP, Luthi A. Neuronal circuits for fear and anxiety. *Nat Rev Neurosci.* 2015; 16:317–331. [PubMed: 25991441]
25. Duvarci S, Bauer EP, Pare D. The bed nucleus of the stria terminalis mediates inter-individual variations in anxiety and fear. *J Neurosci.* 2009; 29:10357–10361. [PubMed: 19692610]
26. Kim SY, Adhikari A, Lee SY, Marshel JH, Kim CK, Mallory CS, et al. Diverging neural pathways assemble a behavioural state from separable features in anxiety. *Nature.* 2013; 496:219–223. [PubMed: 23515158]
27. Botta P, Demmou L, Kasugai Y, Markovic M, Xu C, Fadok JP, et al. Regulating anxiety with extrasynaptic inhibition. *Nat Neurosci.* 2015; 18:1493–1500. [PubMed: 26322928]
28. Shackman AJ, Fox AS, Oler JA, Shelton SE, Davidson RJ, Kalin NH. Neural mechanisms underlying heterogeneity in the presentation of anxious temperament. *Proc Natl Acad Sci U S A.* 2013; 110:6145–6150. [PubMed: 23538303]
29. Fox AS, Oler JA, Shackman AJ, Shelton SE, Raveendran M, McKay DR, et al. Intergenerational neural mediators of early-life anxious temperament. *Proceedings of the National Acadademy of Sciences USA.* 2015; 112:9118–9122.
30. Fox NA, Henderson HA, Marshall PJ, Nichols KE, Ghera MM. Behavioral inhibition: linking biology and behavior within a developmental framework. *Annu Rev Psychol.* 2005; 56:235–262. [PubMed: 15709935]
31. Gibbs RA, Rogers J, Katze MG, Bumgarner R, Weinstock GM, Mardis ER, et al. Evolutionary and biomedical insights from the rhesus macaque genome. *Science.* 2007; 316:222–234. [PubMed: 17431167]
32. Preuss, TM. Primate brain evolution in phylogenetic context. In: Kaas, JH., Preuss, TM., editors. *Evolution of Nervous Sytems.* Vol. 4. Elsevier; NY: 2007. p. 3-34.
33. Fox AS, Oler JA, Tromp DP, Fudge JL, Kalin NH. Extending the amygdala in theories of threat processing. *Trends Neurosci.* 2015; 38:319–329. [PubMed: 25851307]
34. deCampo DM, Fudge JL. Amygdala projections to the lateral bed nucleus of the stria terminalis in the macaque: comparison with ventral striatal afferents. *J Comp Neurol.* 2013; 521:3191–3216. [PubMed: 23696521]
35. Kalin NH, Shelton SE. Defensive behaviors in infant rhesus monkeys: environmental cues and neurochemical regulation. *Science.* 1989; 243:1718–1721. [PubMed: 2564702]
36. Rilling JK, Winslow JT, O'Brien D, Gutman DA, Hoffman JM, Kilts CD. Neural correlates of maternal separation in rhesus monkeys. *Biol Psychiatry.* 2001; 49:146–157. [PubMed: 11164761]
37. Kalin NH, Shelton SE, Fox AS, Rogers J, Oakes TR, Davidson RJ. The serotonin transporter genotype is associated with intermediate brain phenotypes that depend on the context of eliciting stressor. *Mol Psychiatry.* 2008; 13:1021–1027. [PubMed: 18414408]
38. Jahn AL, Fox AS, Abercrombie HC, Shelton SE, Oakes TR, Davidson RJ, et al. Subgenual prefrontal cortex activity predicts individual differences in hypothalamic-pituitary-adrenal activity across different contexts. *Biol Psychiatry.* 2010; 67:175–181. [PubMed: 19846063]
39. Oler JA, Fox AS, Shelton SE, Christian BT, Murali D, Oakes TR, et al. Serotonin transporter availability in the amygdala and bed nucleus of the stria terminalis predicts anxious temperament and brain glucose metabolic activity. *J Neurosci.* 2009; 29:9961–9966. [PubMed: 19675230]



40. Preacher KJ, Rucker DD, MacCallum RC, Nicewander WA. Use of the extreme groups approach: A critical reexamination and new recommendations. *Psychol Methods*. 2005; 10:178–192. [PubMed: 15998176]
41. Kalin NH, Shelton SE, Davidson RJ. Role of the primate orbitofrontal cortex in mediating anxious temperament. *Biol Psychiatry*. 2007; 62:1134–1139. [PubMed: 17643397]
42. Kalin NH, Shelton SE, Davidson RJ. The role of the central nucleus of the amygdala in mediating fear and anxiety in the primate. *J Neurosci*. 2004; 24:5506–5515. [PubMed: 15201323]
43. Chronis-Tuscano A, Degnan KA, Pine DS, Perez-Edgar K, Henderson HA, Diaz Y, et al. Stable early maternal report of behavioral inhibition predicts lifetime social anxiety disorder in adolescence. *J Am Acad Child Adolesc Psychiatry*. 2009; 48:928–935. [PubMed: 19625982]
44. Nichols T, Brett M, Andersson J, Wager T, Poline JB. Valid conjunction inference with the minimum statistic. *Neuroimage*. 2005; 25:653–660. [PubMed: 15808966]
45. Birn RM, Shackman AJ, Oler JA, Williams LE, McFarlin DR, Rogers GM, et al. Evolutionarily-conserved dysfunction of prefrontal-amygdalar connectivity in early-life anxiety. *Mol Psychiatry*. 2014; 19:915–922. [PubMed: 24863147]
46. Davis M, Whalen PJ. The amygdala: vigilance and emotion. *Mol Psychiatry*. 2001; 6:13–34. [PubMed: 11244481]
47. Walker DL, Davis M. Role of the extended amygdala in short-duration versus sustained fear: a tribute to Dr. Lennart Heimer *Brain Struct Funct*. 2008; 213:29–42.
48. Nagy FZ, Pare D. Timing of impulses from the central amygdala and bed nucleus of the stria terminalis to the brain stem. *J Neurophysiol*. 2008; 100:3429–3436. [PubMed: 18971295]
49. Somerville LH, Whalen PJ, Kelley WM. Human bed nucleus of the stria terminalis indexes hypervigilant threat monitoring. *Biol Psychiatry*. 2010; 68:416–424. [PubMed: 20497902]
50. Straube T, Mentzel HJ, Miltner WHR. Waiting for spiders: Brain activation during anticipatory anxiety in spider phobics. *Neuroimage*. 2007; 37:1427–1436. [PubMed: 17681799]
51. Yassa MA, Hazlett RL, Stark CE, Hoehn-Saric R. Functional MRI of the amygdala and bed nucleus of the stria terminalis during conditions of uncertainty in generalized anxiety disorder. *J Psychiatr Res*. 2012; 46:1045–1052. [PubMed: 22575329]
52. Munsterkotter AL, Notzon S, Redlich R, Grotegerd D, Dohm K, Arolt V, et al. Spider or no spider? Neural correlates of sustained and phasic fear in spider phobia. *Depress Anxiety*. in press.
53. Kalin NH, Shelton SE, Fox AS, Oakes TR, Davidson RJ. Brain regions associated with the expression and contextual regulation of anxiety in primates. *Biol Psychiatry*. 2005; 58:796–804. [PubMed: 16043132]
54. Somerville LH, Wagner DD, Wig GS, Moran JM, Whalen PJ, Kelley WM. Interactions between transient and sustained neural signals support the generation and regulation of anxious emotion. *Cereb Cortex*. 2013; 23:49–60. [PubMed: 22250290]
55. McMenamin BW, Langeslag SJ, Sirbu M, Padmala S, Pessoa L. Network organization unfolds over time during periods of anxious anticipation. *J Neurosci*. 2014; 34:11261–11273. [PubMed: 25143607]
56. Alvarez RP, Kirlic N, Misaki M, Bodurka J, Rhudy JL, Paulus MP, et al. Increased anterior insula activity in anxious individuals is linked to diminished perceived control. *Translational psychiatry*. 2015; 5:e591. [PubMed: 26125154]
57. Buss KA. Which fearful toddlers should we worry about? Context, fear regulation, and anxiety risk. *Dev Psychol*. 2011; 47:804–819. [PubMed: 21463035]
58. Wolitzky-Taylor K, Vrshek-Schallhorn S, Waters AM, Mineka S, Zinbarg R, Ornitz E, et al. Adversity in early and mid-adolescence is associated with elevated startle responses to safety cues in late adolescence. *Clin Psychol Sci*. 2014; 2:202–213. [PubMed: 25473591]
59. Craske MG, Wolitzky-Taylor KB, Mineka S, Zinbarg R, Waters AM, Vrshek-Schallhorn S, et al. Elevated responding to safe conditions as a specific risk factor for anxiety versus depressive disorders: evidence from a longitudinal investigation. *J Abnorm Psychol*. 2012; 121(2):315–324. [PubMed: 21988452]
60. Lenaert B, Boddez Y, Griffith JW, Vervliet B, Schruers K, Hermans D. Aversive learning and generalization predict subclinical levels of anxiety: a six-month longitudinal study. *J Anxiety Disord*. 2014; 28(8):747–753. [PubMed: 25254930]



61. LeDoux, JE. *Anxious. Using the brain to understand and treat fear and anxiety.* Viking; NY: 2015.
62. Mobbs D, Yu R, Rowe JB, Eich H, FeldmanHall O, Dalgleish T. Neural activity associated with monitoring the oscillating threat value of a tarantula. *Proceedings of the National Academy of Sciences USA.* 2010; 107:20582–20586.
63. Grupe DW, Oathes DJ, Nitschke JB. Dissecting the anticipation of aversion reveals dissociable neural networks. *Cereb Cortex.* 2013; 23:1874–1883. [PubMed: 22763169]
64. Choi JM, Padmala S, Pessoa L. Impact of state anxiety on the interaction between threat monitoring and cognition. *Neuroimage.* 2012; 59:1912–1923. [PubMed: 21939773]
65. Klumbers F, Kroes MC, Heitland I, Everaerd D, Akkermans SE, Oosting RS, et al. Dorsomedial prefrontal cortex mediates the impact of serotonin transporter linked polymorphic region genotype on anticipatory threat reactions. *Biol Psychiatry.* 2015; 78:582–589. [PubMed: 25444169]
66. Fox AS, Shelton SE, Oakes TR, Converse AK, Davidson RJ, Kalin NH. Orbitofrontal cortex lesions alter anxiety-related activity in the primate bed nucleus of stria terminalis. *J Neurosci.* 2010; 30:7023–7027. [PubMed: 20484644]
67. Shackman AJ, Salomons TV, Slagter HA, Fox AS, Winter JJ, Davidson RJ. The integration of negative affect, pain and cognitive control in the cingulate cortex. *Nat Rev Neurosci.* 2011; 12:154–167. [PubMed: 21331082]
68. Mobbs D, Hagan CC, Dalgleish T, Silston B, Prevost C. The ecology of human fear: survival optimization and the nervous system. *Front Neurosci.* 2015; 9:55. [PubMed: 25852451]
69. McLean CP, Asnaani A, Litz BT, Hofmann SG. Gender differences in anxiety disorders: prevalence, course of illness, comorbidity and burden of illness. *J Psychiatr Res.* 2011; 45:1027–1035. [PubMed: 21439576]
70. Gater R, Tansella M, Korten A, Tiemens BG, Mavreas VG, Olatawura MO. Sex differences in the prevalence and detection of depressive and anxiety disorders in general health care settings: report from the World Health Organization Collaborative Study on Psychological Problems in General Health Care. *Arch Gen Psychiatry.* 1998; 55:405–413. [PubMed: 9596043]
71. Avery SN, Clauss JA, Blackford JU. The human BNST: Functional role in anxiety and addiction. *Neuropsychopharmacology.* 2016; 41:126–141. [PubMed: 26105138]
72. Mai, JK., Paxinos, G., Voss, T. *Atlas of the human brain.* 3. Academic Press; San Diego, CA: 2007.
73. Paxinos, G., Huang, X., Petrides, M., Toga, A. *The rhesus monkey brain in stereotaxic coordinates.* 2. Academic Press; San Diego: 2009.
74. Avery SN, Clauss JA, Winder DG, Woodward N, Heckers S, Blackford JU. BNST neurocircuitry in humans. *Neuroimage.* 2014; 91:311–323. [PubMed: 24444996]
75. Torrisi S, O’Connell K, Davis A, Reynolds R, Balderston N, Fudge JL, et al. Resting state connectivity of the bed nucleus of the stria terminalis at ultra-high field. *Hum Brain Mapp.* 2015; 36:4076–4088. [PubMed: 26178381]
76. Klein A, Andersson J, Ardekani BA, Ashburner J, Avants B, Chiang MC, et al. Evaluation of 14 nonlinear deformation algorithms applied to human brain MRI registration. *Neuroimage.* 2009; 46:786–802. [PubMed: 19195496]
77. Caspi A, Roberts BW, Shiner RL. Personality development: stability and change. *Annu Rev Psychol.* 2005; 56:453–484. [PubMed: 15709943]
78. Gross JJ, Sutton SK, Ketelaar T. Relations between affect and personality: Support for the affect-level and affective reactivity views. *Personality and Social Psychology Bulletin.* 1998; 24:279–288.
79. Suls J, Martin R. The daily life of the garden-variety neurotic: Reactivity, stressor exposure, mood spillover, and maladaptive coping. *J Pers.* 2005; 73:1485–1509. [PubMed: 16274443]
80. Bolger N, Schilling EA. Personality and the problems of everyday life: the role of neuroticism in exposure and reactivity to daily stressors. *J Pers.* 1991; 59:355–386. [PubMed: 1960637]
81. Luck, SJ. Ten simple rules for designing ERP experiments. In: Handy, TC., editor. *Event-related potentials: A methods handbook.* MIT Press; Cambridge, MA: 2005. p. 17-32.
82. Shackman AJ, Sarinopoulos I, Maxwell JS, Pizzagalli DA, Lavric A, Davidson RJ. Anxiety selectively disrupts visuospatial working memory. *Emotion.* 2006; 6:40–61. [PubMed: 16637749]

83. Crapse TB, Sommer MA. Corollary discharge across the animal kingdom. *Nat Rev Neurosci.* 2008; 9:587–600. [PubMed: 18641666]
84. Maren S, Phan KL, Liberzon I. The contextual brain: implications for fear conditioning, extinction and psychopathology. *Nat Rev Neurosci.* 2013; 14:417–428. [PubMed: 23635870]

Author Manuscript

Author Manuscript

Author Manuscript

Author Manuscript

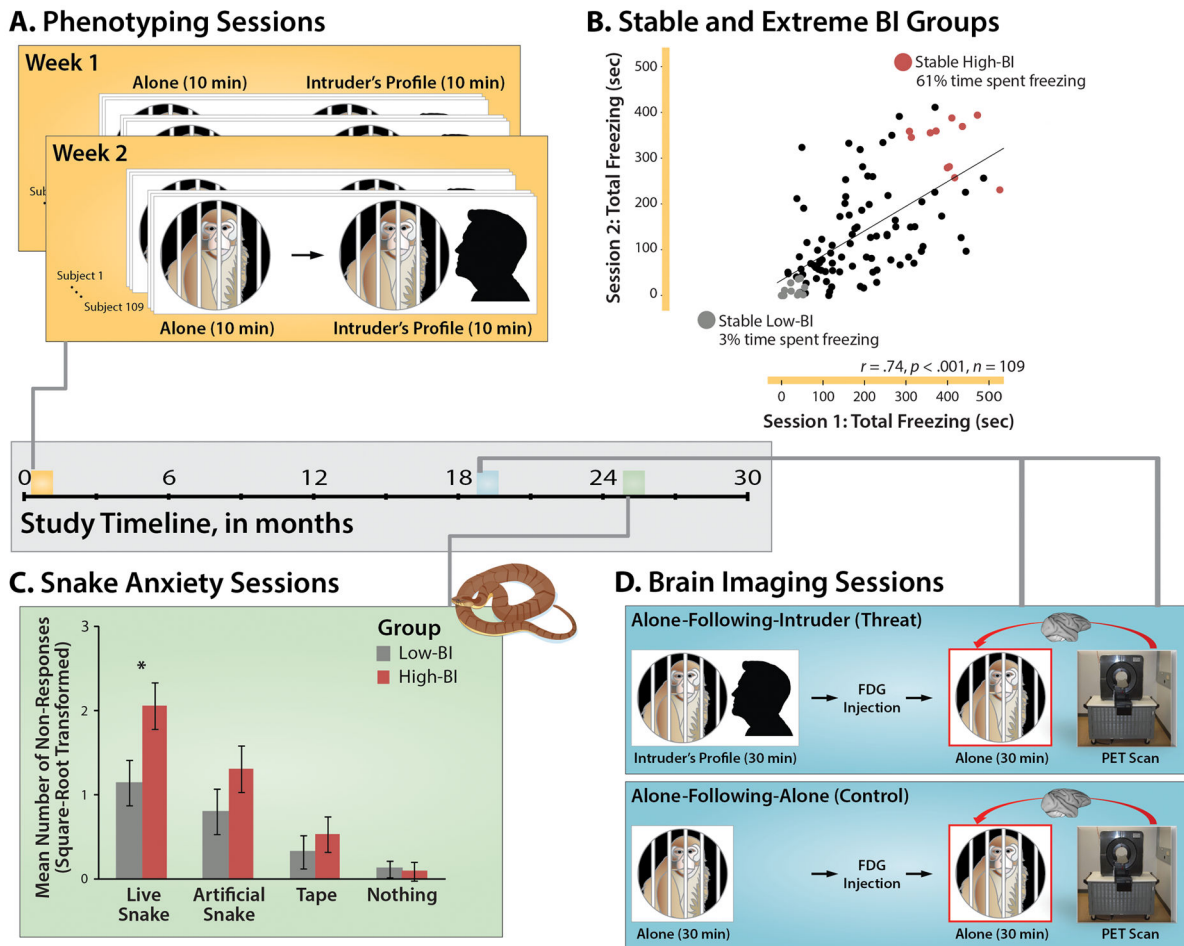


**Figure 1. Overview of longitudinal phenotyping and brain imaging procedures**

The horizontal axis at the center of the figure depicts the relative timing of the longitudinal assessments. **A. Phenotyping sessions.** Individual differences in freezing elicited by diffuse threat (i.e. 10 min exposure to the testing cage) and potential threat (i.e. 10 min exposure to the human intruder's profile) were assessed in 109 monkeys twice, one week apart using the 'Alone' and 'No Eye Contact' conditions of the Human Intruder Paradigm<sup>7, 35</sup>. The Alone condition was always administered first to circumvent carry-over from the higher-intensity intruder challenge. **B. Formation of stable and extreme BI groups.** Groups were formed from individuals who consistently showed extreme freezing in response to the intruder's profile across the two phenotyping sessions. Age- and sex-matched High-BI and Low-BI groups are depicted in red and gray, respectively. For illustrative purposes, the  $x$ - and  $y$ -axes indicate the total number of seconds spent freezing during the 10-min intruder challenges. Inferential statistics employed  $\log_{10}$ -transformed freezing. **C. Snake anxiety sessions.** More than 2 years after initial assessment, subjects were trained to retrieve highly-preferred foods in the Wisconsin General Testing Apparatus. During the snake anxiety assessment, foods were placed on top of a clear enclosure containing a live snake, an artificial snake, a roll of tape, or nothing. As shown in the bar plot, the stable High-BI group shows significantly greater passive avoidance in the presence of the live snake (Group  $\times$  Stimulus,  $p < .05$ ).

Asterisk indicates significant pairwise group difference. Error bars depict SE. **D. Brain imaging sessions.** Approximately 1.5 years after the initial assessment, subjects were scanned. FDG-PET scanning was conducted in two sessions (order pseudo-randomized). Subjects were acclimated to behavioral testing procedures for 5 days prior to the first scanning session. In the threat condition (upper blue panel), subjects were placed in a testing cage and exposed to the human intruder's profile for 30-min. To minimize habituation, the intruder presented his profile for 10 min, exited the testing environment, returned after 5 min, presented his profile for 5 min, exited for 5 min, and then presented for a final 5 min. At the end of the 30-min challenge, subjects received an injection of the radiotracer  $^{18}\text{F}$ FDG and were returned to the testing cage. At the end of this 30-min 'recovery' period, subjects were anesthetized and positioned in the high-resolution, small-bore PET scanner. The control condition (lower blue panel) differed only in the absence of threat exposure during the initial 30-min. Comparison of the physically-identical 'recovery' periods of the threat and control conditions (red boxes) enabled us to assess group differences in regional brain activity following the intruder encounter. Portions of this figure were adapted with permission from Refs.<sup>83, 84</sup>.

### The High-BI group shows persistently elevated freezing following the intruder encounter

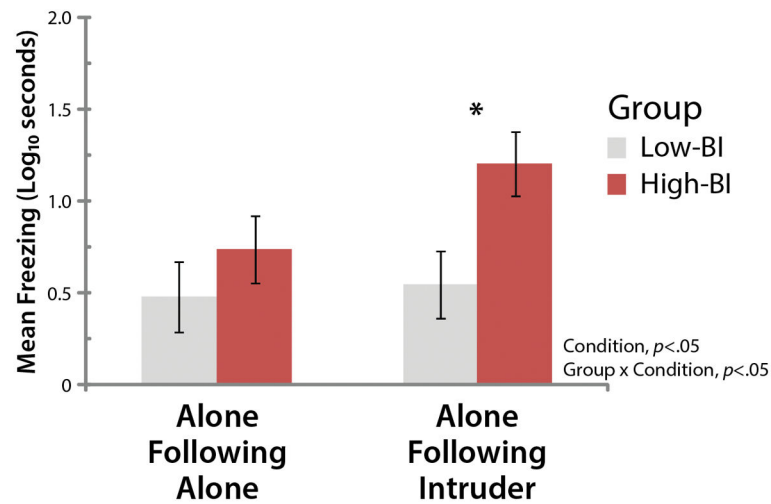


**Figure 2. The stable High-BI group shows persistently elevated freezing during the ‘recovery’ period following the intruder encounter (1.5 years later)**

See Figure 1d for an overview of the paradigm. The groups did not significantly differ in the Alone-Following-Alone control condition ( $p=.35$ ). The High-BI group froze longer following the encounter (Alone-Following-Intruder) compared to the control condition (Alone-Following-Alone) ( $F(1,21)=12.04$ ,  $p=.002$ ). The  $y$ -axis indicates the log<sub>10</sub>-transformed freezing duration, averaged across six consecutive 5-min bins. Asterisk indicates significant pairwise group differences. Error bars depict SE.

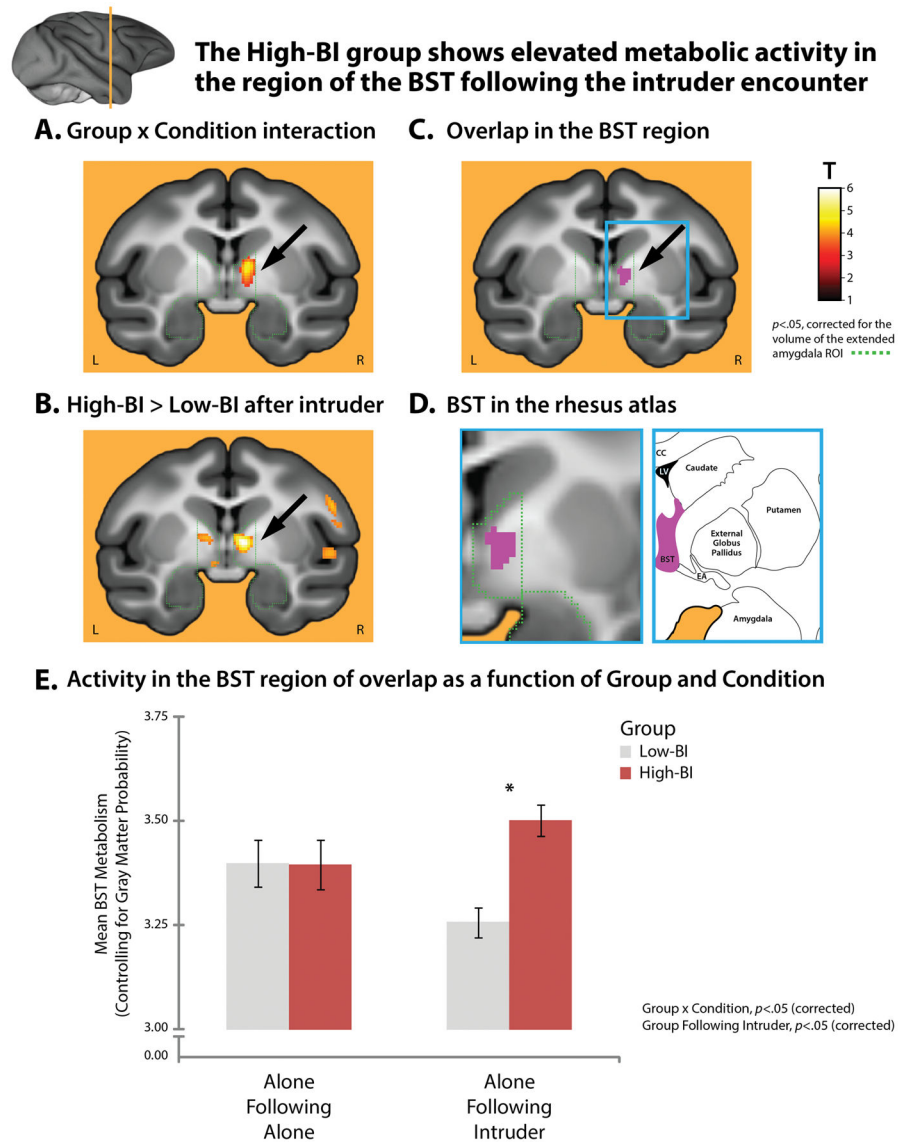


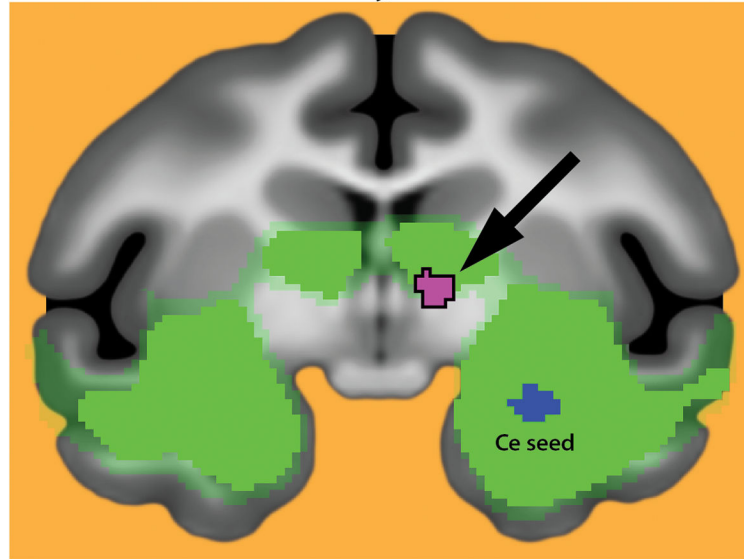
**Figure 3. The High-BI group shows elevated metabolic activity in the region of the BST following the intruder encounter**

The *a priori* extended amygdala ROI is indicated by the dashed green line. The imaging paradigm is depicted in Figure 1d. **A. Regions showing a significant Group  $\times$  Condition interaction.** The cluster in the region of the BST is indicated by the black arrow ( $p < .05$ , small-volume corrected). Data extracted from this cluster is depicted in Supplementary Figure S1. **B. Regions where the stable High-BI group showed significantly more activity than the Low-BI group during the 30-min ‘recovery’ period following the intruder encounter.** Clusters visually depicted outside the ROI (green) were not significant using a whole-brain threshold. **C. Region of overlap in the BST region.** A minimum conjunction<sup>44</sup> (logical AND) of the whole-brain contrasts shown in panels A and B revealed a cluster in the vicinity of the BST (purple). No other clusters were identified. **D. BST in the corresponding region of the rhesus brain atlas.** The left image shows a magnified view of the region marked by the cyan rectangle in panel C. The arrow is omitted for clarity. The

right image depicts corresponding region of the rhesus atlas. Additional views of the BST clusters can be found in Supplementary Figure S2. **E. Activity in the BST region of overlap as a function of Group and Condition.** Figure shows mean activity from the purple cluster depicted in panel C controlling for nuisance variance in mean-centered gray matter probability. Asterisk indicates the significant pairwise group differences. Error bars depict SE. Portions of this figure were adapted with permission from plate 54 in the atlas of Paxinos and colleagues<sup>73</sup>. **Abbreviations**—CC: corpus callosum, EA: extended amygdala, LV: lateral ventricle.



**Multimodal imaging reveals that the region identified by FDG-PET overlaps with a region showing high levels of Ce functional connectivity, consistent with the BST**



Overlap between regions identified using FDG-PET and fMRI

■ 3-way minimum conjunction of 'Group x Condition,'  
'High-BI > Low-BI after Intruder,' and Ce functional connectivity

Ce intrinsic functional connectivity (fMRI)

■ Connectivity,  $t > 8.5$  }  $N = 89, p < .005$  whole-brain Šidák corrected  
 ■ Connectivity,  $t > 6.5$  }

**Figure 4. Multimodal imaging reveals that the hypermetabolic region identified by FDG-PET overlaps a region expressing high levels of Ce functional connectivity, consistent with the BST** Shown in purple is the overlap (i.e. minimum conjunction<sup>44</sup>) between voxels identified using FDG-PET (purple cluster in Figure 3c) and those showing significant functional connectivity with the Ce (green) in an independent sample of 89 monkeys (detailed in Ref. <sup>45</sup>). The substantial overlap enhances our confidence that the hyper-metabolic region identified using PET encompasses portions of the BST. The Ce seed region used in the functional connectivity analyses is depicted in blue.

**Table 1**

Descriptive statistics for the extreme behavioral inhibition (BI) groups.

<u>Age (Years)<sup>c</sup></u>	<u>High-BI<sup>a</sup></u>		<u>Low-BI<sup>b</sup></u>	
	<u>M</u>	<u>SD</u>	<u>M</u>	<u>SD</u>
First screening session	2.31	.57	2.14	.53
First FDG-PET session	3.94	.60	3.76	.56
Second FDG-PET session	3.99	.60	3.80	.57
Snake anxiety assessment	4.45	.62	4.26	.56

<sup>a</sup>Consisted of 8 females and 3 males.

<sup>b</sup>Consisted of 9 females and 3 males.

<sup>c</sup>The groups did not differ in sex or age,  $p > .44$ .

Author Manuscript

Author Manuscript

Author Manuscript

Author Manuscript